Vibrational Spectroscopy on pDTT3 A Low Band Gap Polymer Based on Dithienothiophene

ARTICLE *in* THE JOURNAL OF PHYSICAL CHEMISTRY B · JANUARY 2001

Impact Factor: 3.3 · DOI: 10.1021/jp0020586

Vibrational Spectroscopy on pDTT3−A Low Band Gap Polymer Based on Dithienothiophene

Antonio Cravino,[†] Helmut Neugebauer,*[,†] Silvia Luzzati,[‡] Marinella Catellani,[‡] and N. Serdar Sariciftci[†]

Physical Chemistry, Johannes Kepler University Linz, Altenbergerstrasse 69, A-4040 Linz, Austria, and Istituto di Chimica delle Macromolecole, CNR, Via Bassini 15, I-20133 Milano, Italy

Received: June 7, 2000; In Final Form: October 10, 2000

Attenuated total reflection Fourier transform infrared studies of the electrochemical redox processes of poly(dithieno[3,4-b:2′,3′-d]thiophene) (pDTT3), a low band gap conjugated polymer with a "polythiophene-like" backbone, where an aromatic moiety is fused to each thiophene ring, are reported. Vibrational spectroscopic studies are performed in situ during electrochemical oxidation (*p*-doping) and reduction (*n*-doping). Infrared active vibration bands due to charge carriers injected to the polymer chain are compared to photoinduced IR bands and to Raman spectra of the neutral polymer. The similar spectral features, observed during *p*- and *n*-doping processes, indicate a high charge carrier delocalization for both signs of carriers. Furthermore, the spectral evidence of the strong involvement of the fused aromatic rings to the π-electronic structure of this low band gap polymer has been obtained.

1. Introduction

Infrared and Raman spectroscopy have been used as complementary methods to study conjugated polymers that show strong electron−phonon coupling due to their quasi one-dimensional structure. Redox processes in conjugated polymers that lead to oxidized or reduced conducting states with mobile charge carriers are commonly accompanied by a strong relaxation of the one-dimensional lattice geometry around these charged defects. In analogy to inorganic semiconductors, these redox processes, which lead from semiconducting conjugated states into metallically conducting states, are described as *p*- or *n*-doping. The charge carriers, with their indigenous lattice relaxation, are described, such as polarons. The magnitude of the electron/phonon coupling constant as well as the effective conjugation has been used to account for the degree of the lattice relaxation in conjugated polymers.

The infrared spectra of conjugated polymers exhibit, upon doping, new and very intense infrared active vibration (IRAV) bands correlated to the strong electron−phonon coupling. In addition, broad and strong absorption bands with energies less than the semiconductor absorption edge are observed and related to in-the-gap states created by the polaronic relaxation.[1] With Amplitude Mode (AM) formalism, Horovitz et al. have presented a model to explain IRAV bands in doped polyacetylene.[2,3] In this formalism, IRAV bands are determined by the coupling of electronic excitations to the so-called "amplitude oscillation", which describes the influence of the excitation on the single and double bond length alternation along the polymer backbone (a concept based on the Su−Schrieffer−Heeger model[4,5]). Zerbi et al. showed the correlation between IRAV bands of conjugated polymers and the IR activation of totally symmetric A_g modes which contain a contribution of the so-called "effective conjugation coordinate" (ECC theory).[6,7] This coordinate describes the geometrical changes, going from the ground state to the excited state of the polymer, as a collective stretching-shrinking of carbon−carbon bonds. From the participation of A_g modes, it is evident that Raman spectra are of high importance for the description of vibrational properties in systems with electron−phonon coupling and for the understanding of the nature of IRAV bands in conjugated polymers. The ECC theory can be applied to all polymers that possess a well defined effective conjugation coordinate. Both approaches[8] have been adapted to polyaromatic and polyheteroaromatic conjugated polymers like polypyrrole and polythiophene, including some derivatives. More recently, a model that introduces a link between the doping induced electronic states within the electronic band gap and the IRAV bands has been proposed by Ehrenfreund and Vardeny.[9] In all of these models, there is a strong relation between the effective conjugation length in the macromolecule, the effective delocalization of the doping induced quasi particles, and the IRAV signature in the infrared spectrum.

Among conjugated polymers, polythiophenes have attracted large attention, both in experimental and theoretical work, because of their electrical and optical properties and relatively simple chemical structures. Experimentally, doping can be performed either by chemical or electrochemical oxidation (*p*-doping) and reduction (*n*-doping) or by photoexcitation (photodoping). The infrared spectra of the oxidized or photoexcited forms of polythiophene exhibit, in the range from 1600 to 600 cm^{-1}, three strong IRAV bands[6,7,10,11] related to three main Raman active A_g modes found in the neutral form of the polymer.[12] Substitution with alkyl or alkyloxy side chains gives an additional Raman active A_g mode at about 1000 cm^{-1} and, consequently, an additional activated band in the IRAV range.[13] In the theories mentioned above, the polymers are considered "pseudopolyenes". Despite such a strong simplification, the models provide a self-consistent picture for PT and other thiophene based conjugated polymers. The presence of additional weak peaks has been explained by side groups effects

* To whom correspondence should be addressed. Fax: +43-732-2468-8770. E-mail: helmut.neugebauer@jk.uni-linz.ac.at.
[†] Physical Chemistry, Johannes Kepler University Linz.
[‡] Istituto di Chimica delle Macromolecole, CNR.

10.1021/jp0020586 CCC: $20.00
Published on Web 12/09/2000

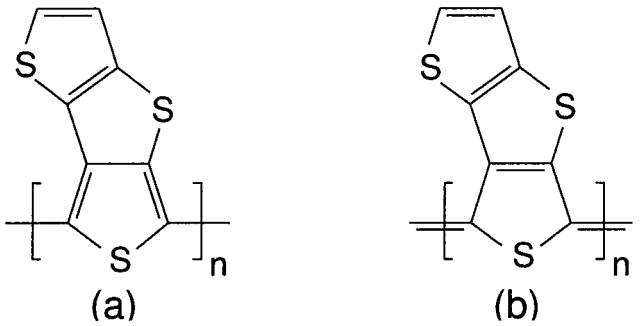

Figure 1. Chemical structure of pDTT3. (a) and (b) are two resonance structures.

("shape modes" in the AM formalism, as developed by Mele and Hicks[14]), and by polydispersivity in effective conjugation lengths.[7] In the photoinduced IR spectrum of polythiophene, Schaffer and Heeger have observed the activation of weak features that were assigned to ring vibrations containing C−S stretching contributions ("ring modes").[15] These vibrations are not directly related to the dimerized, pseudopolyenic part of the polymer chain. The importance of heteroatoms in determining the vibrational spectra has been recently discussed by Agosti et al., who have reanalyzed data obtained from many thiophene derivative-based conjugated polymers.[16] Significant spectral features, related to ring modes and to the presence of heteroatoms, should be expected for more complex structures, especially when substituents or fused rings strongly influence the electronic properties of the polymer.

Complex systems as thiophene-based fused ring polymers are promising candidates for applications because they have low electronic $\pi \rightarrow \pi^*$ band gap and unusual optical properties.[17−21] Poly(dithieno[3,4-b:2′,3′-d]thiophene) (pDTT3) is a conjugated polymer consisting of dithienothiophene units (monomer composed of three fused thiophene rings) in which the β-fused thiophene of each repeating unit takes part in the polymeric backbone with $\alpha-\alpha'$ branching.[22,23] The structure is shown in Figure 1. pDTT3 has an electronic band gap of 1.05 eV, which is among the lowest values reported until now.[18] This property, associated with the fact that the polymer undergoes both reversible electrochemical oxidation and reduction in organic electrolytes, makes the material highly interesting for various applications such as redox capacitors, or electrochromic and photovoltaic devices. A detailed electrochemical characterization of the polymer has been reported by Arbizzani et al.[24] In general, variations in the size of the electronic band gap in conjugated polymers result from many parameters such as steric effects and nature of the substituents.[18] In pDTT3, the fusion of heteroaromatic rings with a high π-electron delocalization appears to be the main cause of the unusual small gap, which is about 0.7 eV smaller than in high quality, regioregular polyalkylthiophenes.[25−27]

From a study of the vibrational behavior, information on the interaction of fused heteroaromatic rings with the π-electron delocalization along the "polythiophene-like" polymeric backbone can be obtained. In this paper, we present results on in situ attenuated total reflection (ATR) FTIR spectroelectrochemistry during oxidation (*p*-doping) and reduction (*n*-doping) of pDTT3 in organic electrolytes. The spectra are compared to photoinduced IR absorption spectra and to Raman spectra of neutral pDTT3. The results confirm a strong influence of the fused moiety to the vibrational and electronic properties of pDTT3 as well as a very similar relaxation pattern for the doping induced charge carriers of both signs.

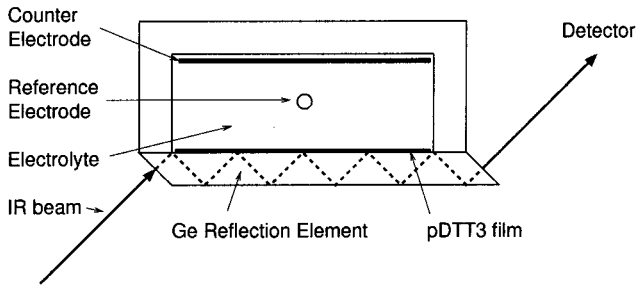

Figure 2. Spectroelectrochemical cell for in situ ATR-FTIR spectroscopy.

2. Experimental Section

The monomer dithieno[3,4-b:2′,3′-d]thiophene (DTT3) was synthesized following a method published in the literature.[28] Details on the electrosynthesis and the electrocharacterization of the polymer pDTT3 have been already reported.[24] In the present work, films of the polymer were prepared electrochemically in the spectroelectrochemical cell schematically shown in Figure 2. The electrode consisted of a germanium reflection element coated with a thin evaporated layer of platinum, with an electrochemically active area of 0.63 cm^2. For the polymerization, as well as for the in situ spectroelectrochemical investigations, the electrolyte was 0.1 M tetrabutylammonium-hexafluorophosphate (dried at 180 °C under vacuum) in acetonitrile (Selectipur-Merck, stored over molecular sieve). The electrolyte solution was prepared and kept under argon flow to exclude moisture and oxygen during the electrochemical processes. The monomer solution was prepared in dry argon atmosphere using shielded glassware and then transferred to the spectroelectrochemical cell via syringe. After polymerization, the solution containing the unreacted monomer was removed, and the spectroelectrochemical cell was filled with fresh electrolyte. As counter and reference electrodes a platinum foil and a Ag/AgCl wire quasi electrode were used, respectively. In this work, all of the potential values refer to this reference electrode (determined as −190 mV vs SCE). The electrochemical equipment consisted of a potentiostat (Jaissle 1002T-NC), a sweep generator (Prodis 1/14I) and a X−Y recorder (Rika-denki RY-PIA). The measurements were performed at room temperature. During potential sweeps with a rate of 5 mV/s, FTIR spectra were recorded consecutively. By chosing one spectrum as reference and relating the subsequent spectra to this reference spectrum, specific spectral changes during an electrochemical process are obtained. The difference spectra are calculated as $\Delta(-\log(T_{ATR}))$, where T_{ATR} is the transmittance in the ATR geometry. Each spectrum covers a range of about 85 mV in the cyclic voltammogram. Details on the ATR-FTIR in situ spectroelectrochemistry technique and the setup have been published elsewhere.[29−32]

In addition to spectroelectrochemical ATR-FTIR measurements, photoinduced absorption (PIA) infrared spectra of the same sample in the neutral form were recorded. After spectroelectrochemistry, the polymer film in the neutral form, still on the Ge reflection element, was washed with acetonitrile and dried in an argon laminar flow box. Working in argon atmosphere, the dried film was mounted in a cryostat with ZnSe windows and cooled with liquid nitrogen. The sample was illuminated in 45° geometry through a quartz window by the 488 nm line of an Ar^+ laser (30 mW/cm^2). The photoinduced absorption was observed by measuring a sequence of 300 repetitions of recording 10 coadded single beam spectra under illumination and 10 coadded single beam spectra in the dark.

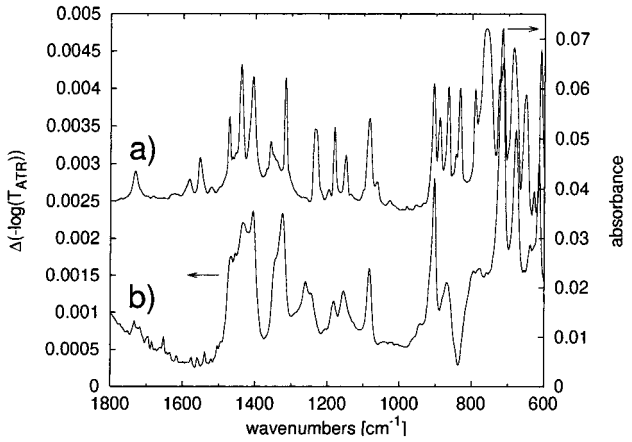

Figure 3. (a) IR spectrum of the monomer DTT3. (b) IR spectrum of neutral pDTT3, obtained in situ at −600 mV using the cell filled with electrolyte solution as reference.

Combining the respective spectra, the photoinduced absorption was calculated as $-\Delta T/T$. For both ATR-FTIR and PIA-FTIR spectroscopy, a Bruker IFS 66S spectrophotometer with a liquid nitrogen cooled MCT detector was used. UV−vis spectroscopy and Raman measurements have been carried out on films electropolymerized on ITO glass (Balzer, resistivity 20 ohms) electrodes and then carefully dedoped. The UV−vis absorption spectra were recorded with a Cary 2400 spectrophotometer. Raman measurements were performed in the near-infrared (NIR) with a Bruker IFS66+FRA106 FT-spectrophotometer working with a Nd:YAG laser (1064 nm) and, in the visible range, with a flat field triple monochromator (Jasco TRS 300) equipped with an EG&G intensified diode array (OMA 1420), using Ar^+ and He−Ne laser lines at 457, 514, and 633 nm. The measurements have been carried out at room temperature, keeping the samples under vacuum. All the infrared and Raman spectra were recorded with a resolution of 4 cm^{-1}.

3. Results and Discussion

3.1. *In situ* FTIR Spectroelectrochemistry. For comparison, the spectrum of the neutral form of pDTT3 was recorded in situ in the spectroelectrochemical cell, in contact with the electrolyte solution and under an applied potential of −600 mV. The spectrum of the cell filled with electrolyte but without polymer film was used as reference. The spectrum is shown in Figure 3b. Frequencies and relative intensities of the IR absorption bands of neutral pDTT3 are reported in Table 1. Figure 3a shows also the IR spectrum of the monomer DTT3.

The development of IRAV bands starts at potentials that coincide with the onset of oxidative or reductive current peaks in the cyclic voltammogram depicted in Figure 4. Figure 5 shows the difference spectra during electrochemical oxidation of pDTT3. In Figure 5a, the spectra are dominated by a broad absorption at high energy, correlated to the formation of new electronic states within the gap, with a maximum around 2800 cm^{-1}. In the vibrational part (Figure 5b), where the IRAV range is shown in detail, a complicated band pattern is growing during the oxidation. The frequencies and characteristics of these bands are collected in Table 2. In the region 950−600 cm^{-1}, where several sharp peaks appear, the band at 842 cm^{-1} is due to the incorporation of hexafluorophosphate counterions, which balance the positive charge formed on the polymer during oxidation. IRAV bands of oxidized pDTT3 show high intensities as expected for modes which have strong electron−phonon coupling. As can be seen by comparing Figures 5b and 3b, the bands of the oxidized form are at least 5 times more intense than the bands of the neutral polymer. Moreover, the main bands in the range from 1500 to 1000 cm^{-1} are broad, which indicates, together with the high intensities, a rather high delocalization of the positive charges along the chain.[6,7]

TABLE 1: IR Bands of Neutral pDTT3[a]

frequency [cm^{-1}]	intensity	comment
1464		shoulder
1432	m	broad
1406	m	
1324	s	
1269		shoulder
1261	m	
1184	w	
1155	w	
1084	m	sharp
903	s	sharp
870	w	
839	s	sharp
715	vs	sharp
678	s	sharp
639	vw	sharp
613	s	sharp

[a] Intensities: vs, very strong; s, strong; m, medium; w, weak; vw, very weak.

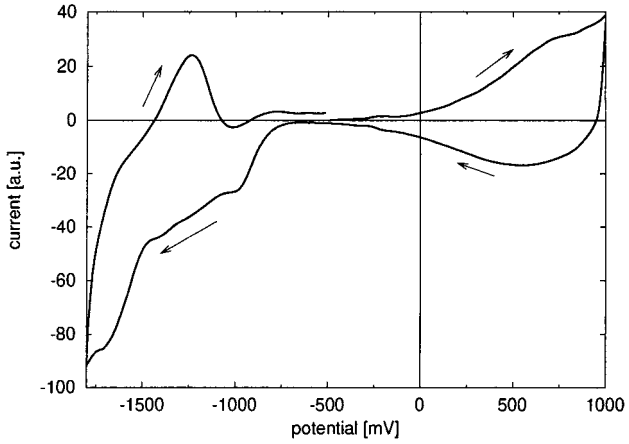

Figure 4. Cyclic voltammogram during the in situ spectroelectrochemical experiment. Electrolyte 0.1 M Bu_4NPF_6 in CH_3CN, sweep rate 5 mV/s.

Among electroactive conjugated polymers, pDTT3 is one of few examples that can be both oxidized and reduced reversibly. The difference ATR-FTIR spectra during electrochemical reduction of the polymer are depicted in Figure 6. The high-energy part of the spectra (Figure 6a) shows a broad absorption, with a maximum that shifts from 3250 to 2800 cm^{-1} with increasing doping level. The IRAV bands that arise during reduction (Figure 6b) give a spectrum similar to the spectrum of the oxidized material. Apart from slight differences in the relative intensities, especially above 1000 cm^{-1} all of the spectral features are present in both spectra of oxidized and reduced pDTT3. The most striking differences are the missing hexafluorophosphate band at 842 cm^{-1} in the reduced polymer and the shift of the peak at 940 cm^{-1}, found for the oxidized form, to 891 cm^{-1} in the reduced pDTT3 spectrum. Again, sharp peaks appear in the region 950−600 cm^{-1}. In contrast to other thiophene-based conjugated polymers,[19,20] the difference spectra of oxidized and reduced pDTT3 exhibit IRAV bands with almost the same intensities. The high similarity between the spectral signatures of oxidized and reduced pDTT3 suggests that the nature of the charge carriers of both signs is very similar. Spectral data from the reduction process, obtained with internal ATR-FTIR in situ

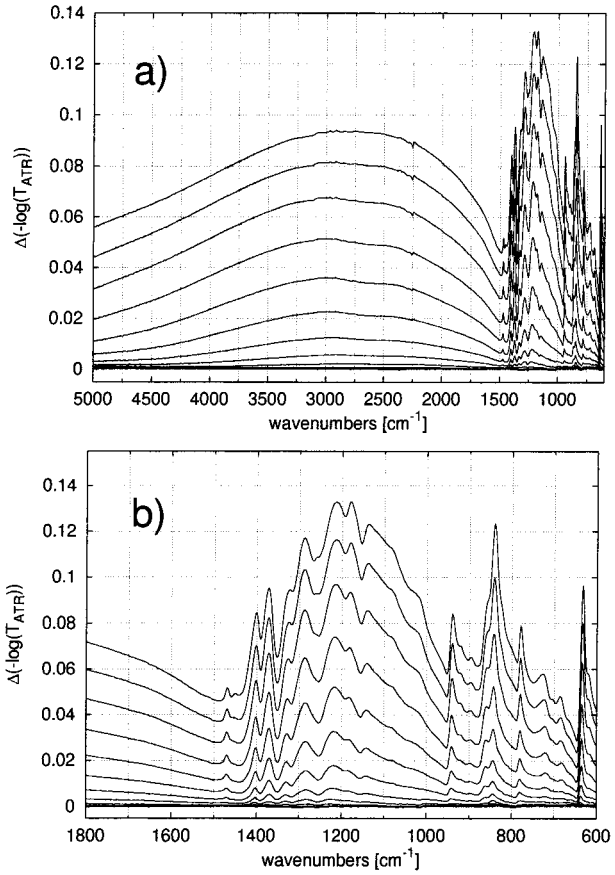

Figure 5. 1R difference spectra of pDTT3 during oxidation. Sequence: bottom to top. (a) extended range; (b) IRAV range.

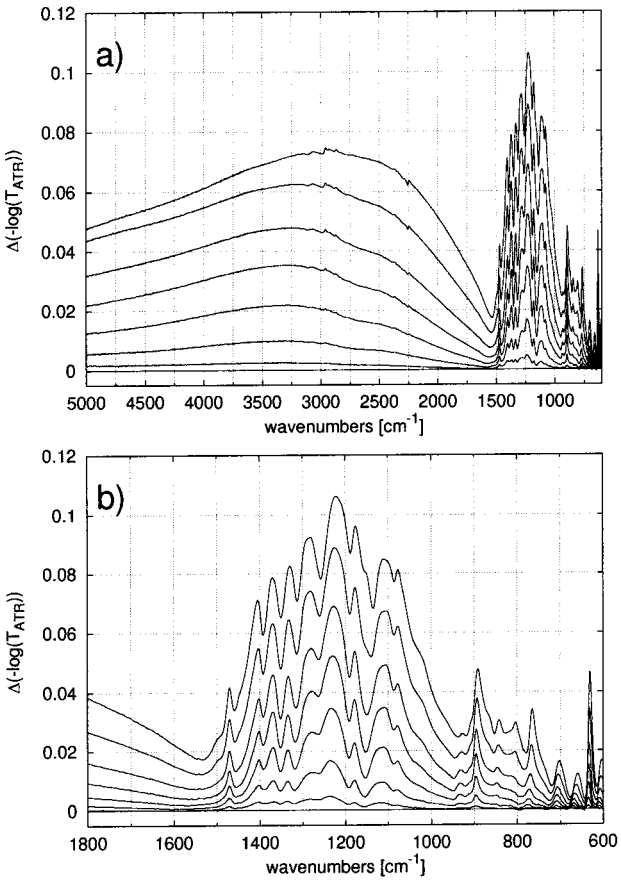

Figure 6. 1R difference spectra of pDTT3 during reduction. Sequence: bottom to top. (a): extended range; (b): IRAV range.

TABLE 2: IR Bands of Doped pDTT3[a]

oxidation		reduction		PIA
1460	w	1469	w	1469
1445	vw			
1401	m	1403	m	1400
1371	m	1369	m	1372
1326	shoulder	1329	m	1330
1287	m	1281	s	1295
1214	s	1221	vs	1226
1180	s	1176	s	1180
1139	s broad	1150	shoulder	1140
		1110	s	
1020	shoulder	1080	m	
940	w			941
		891	m	862
842	vs el sharp			
778	w	764	m	777
721	w	700	w	
684	w	660	w	
634	s sharp	630	s sharp	634

[a] The numbers are wavenumbers: vs, very strong; s, strong; m, medium; w, weak; vw, very weak; el, electrolyte.

spectroelectrochemistry as well as data from PIA-FTIR measurements (will be discussed in the following paragraph) are also listed in Table 2.

3.2. Photoinduced FTIR Spectroscopy. Similarities in the IR spectra of chemical or electrochemical doped and photodoped conjugated polymers have been found for many systems. However, in electrochemically doped material, the counterions introduce a pinning effect of the charge carriers, responsible for the localization of the charged quasi-particles in a relative localized domain. Usually, the absence of counterions in the photodoped material allows higher effective conjugated lengths and, therefore, softening of some vibrations.[33] The photoinduced FTIR spectrum of pDTT3 is depicted in Figure 7. The two derivative-shaped features at about 900 and 710 cm^{-1} are due to heating-induced changes of the corresponding bands in the absorption spectrum of the neutral form of the polymer (Figure 3b). Apart from these features, the spectrum is very similar to the electrochemically induced IR spectrum. Although electrolyte counterions are absent, some kind of pinning must be taken into account, probably due to a formation of deeply trapped charged sites (e.g., chain defects) with long lifetime. A further investigation by time-resolved photoinduced infrared absorption might be useful to achieve a better description of this behavior.

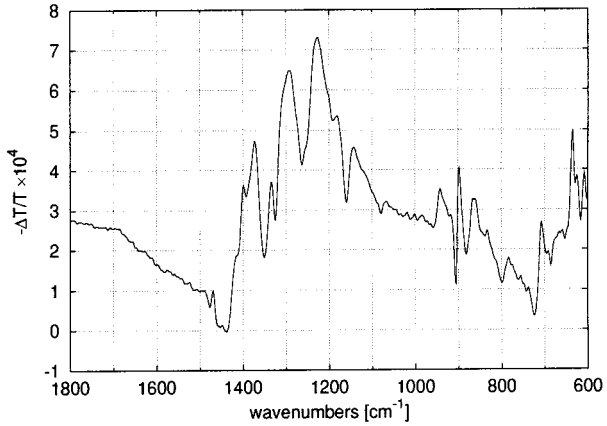

Figure 7. PIA-FTIR spectrum of pDTT3, neutral form. Excitation at 488 nm, 30 mW/cm^2.

3.3. Raman Spectroscopy. For comparison with the FTIR spectroelectrochemical investigations and to determine the

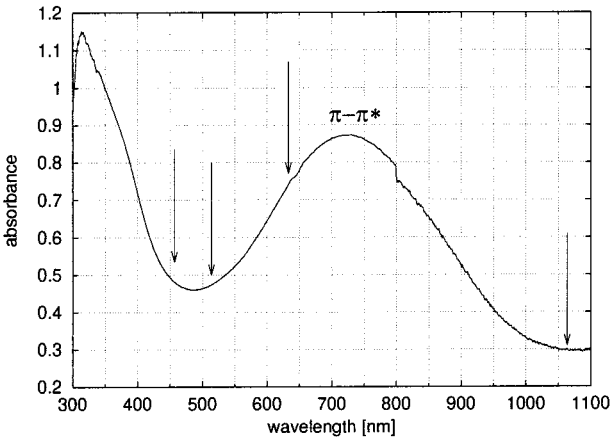

Figure 8. UV−vis spectrum of pDTT3, neutral form. Arrows indicate the excitation wavelengths for Raman measurements.

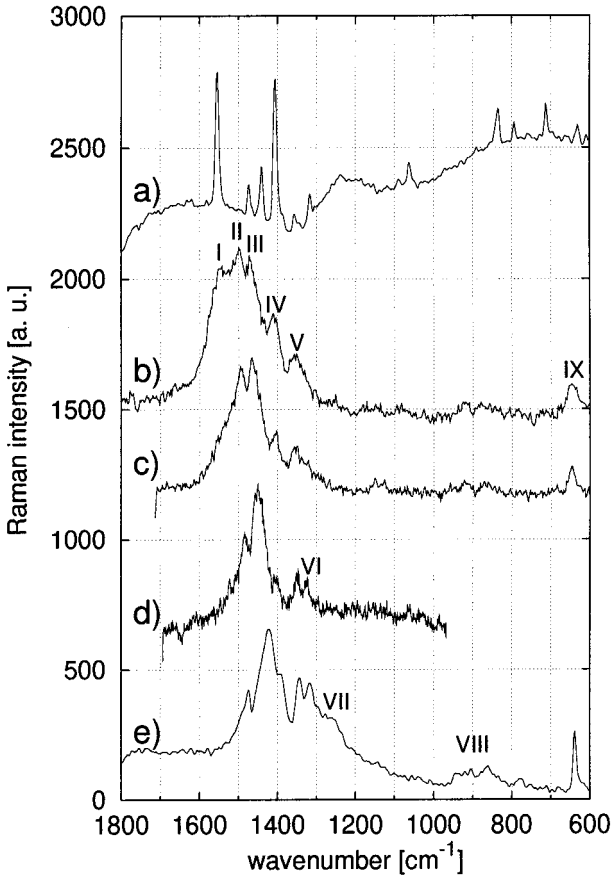

Figure 9. (a) FT-Raman spectra of monomer DTT3, excited at 1064 nm. Raman spectra of neutral pDTT3, excited at (b) 457 nm, (c) 514 nm, (d) 633 nm, (e) 1064 nm. The spectra are rescaled and separated individually.

dependence of the Raman lines on the excitation energy, we carried out Raman scattering measurements, using visible and near-infrared (NIR) excitations. The UV−vis absorption spectrum of the neutral form of pDTT3, with arrows indicating the exciting wavelengths for the Raman studies, is depicted in Figure 8. The absorption peak around 700 nm corresponds to the $\pi \rightarrow \pi^*$ transition of the polymer. The Raman spectra taken with different excitation wavelengths, both in resonance and out of resonance with the $\pi \rightarrow \pi^*$ transition, are shown in Figure 9. The Raman spectrum (NIR excitation) of the monomer DTT3 is also reported in Figure 9a.

The complexity of pDTT3 is shown also by the Raman spectra that contain more features than those of other simpler conjugated polymers. The NIR Raman spectrum of the polymer (Figure 9e) exhibits six main bands at 1475 cm^{-1} (assigned to band number II), 1422 (III), 1344 (V), 1318 (VI) and 639 cm^{-1} (IX); shoulders or broad and weak features are detected at about 1390 (IV), 1270 (VII), and around 900 cm^{-1} (several overlapping bands with low intensities, indicated with VIII). In contrast to results obtained with simpler conjugated polymers, some Raman bands of the polymer coincide with Raman modes of the monomer. The two Raman bands observed at 1547 cm^{-1} (I) and 1407 cm^{-1} (IV) in the spectrum taken with excitation at 457 nm, which is off-resonance with the $\pi \rightarrow \pi^*$ transition (Figure 9b), correspond to two very strong Raman bands of the monomer (Figure 9a). Further coincidences with weaker monomer bands are observed for the modes at 1473 cm^{-1} (III) and 1355 cm^{-1} (V).

The Raman spectra show intensity redistribution with the exciting energy (Figure 9b−e). Going from 457 nm (Figure 9b) to NIR (Figure 9e) excitation, band I disappears and band IV becomes shoulder. This behavior, associated with the already discussed correspondence to two strong Raman modes of the monomer, indicates that these modes are localized within the dithienothiophene moiety. Band III strongly increases in intensity with increasing excitation wavelength and becomes the dominating signal in the Raman spectrum taken with NIR excitation. Other signals that gain in intensity, but have no correspondence to monomer bands, are VI, VII, and VIII. The last two are only clearly seen with NIR excitation. Band II loses intensity but remains noticeable, even exciting with long wavelength (Figure 9e).

Apart from changes in intensity, some bands show also changes in frequency at different excitation energies. Bands II, III, V, and VI decrease in frequency with decreasing excitation energy, i.e., according to the models, by the selective enhancement of longer conjugation lengths.[34] This softening indicates a rather strong electron−phonon coupling for these modes. The largest frequency dispersion, as well as the highest increase in oscillator strength, shows band III, which shifts from 1473 cm^{-1} (Figure 9b) to 1422 cm^{-1} (Figure 9e) with excitation at 457 and 1064 nm, respectively. These features indicate that this vibration, mainly containing C═C stretching contribution, has the highest electron−phonon coupling being delocalized along the polymeric backbone.

3.4. Comparison of in situ IR and Raman Spectra. Despite the complexity discussed above and the broad shape of many signals, correspondences between Raman bands (Figure 9b−e) and IRAV bands of the electrochemically oxidized polymer (Figure 5b) can be found:

- Band II, which decreases and moderately shifts in Raman, corresponds to the weak IR peak at 1460 cm^{-1}.
- The set of bands III, V, and VI, which gain intensity increasing the excitation wavelength, remains intense and shows a further shift (about 30 cm^{-1}) going to the IR spectrum of oxidized pDTT3. Band III seems to split in two bands at 1401 and 1371 cm^{-1}.
- The broad and weak features VII and VIII, emerging in the Raman spectrum with NIR excitation, appear with high intensity in the IR absorption and give the two extended and complicated patterns in the regions 1250−1120 cm^{-1} and 950−770 cm^{-1}. The Raman feature VII seems to be splitted in several broad components.
- A remarkable and particular behavior shows the low-frequency band at about 640 cm^{-1} (IX), which is quite far away from the range commonly considered for IRAV modes. It does not show dispersion and is always quite strong upon changing

TABLE 3: Band Assignment and Wavenumbers of Raman and IRAV Modes[a]

	I	II	III	IV	V	VI	VII	VIII	IX
457 nm	1547	1500	1473	1407	1355				646
514 nm		1495	1466	1402	1353	1331			646
633 nm		1485	1451	1402	1348	1325			
1064 nm		1475	1422		1344	1318	1250 broad	950−770	639
ec		1460	1401		1326	1287	1250−1120	950−770	634
			1371						
PIA		1469	1400		1330	1295	1250−1120	950−770	634
			1372						

[a] Roman numbers are band numbers, wavelength for Raman excitation, ec electrochemical oxidation, PIA photoinduced IR absorption

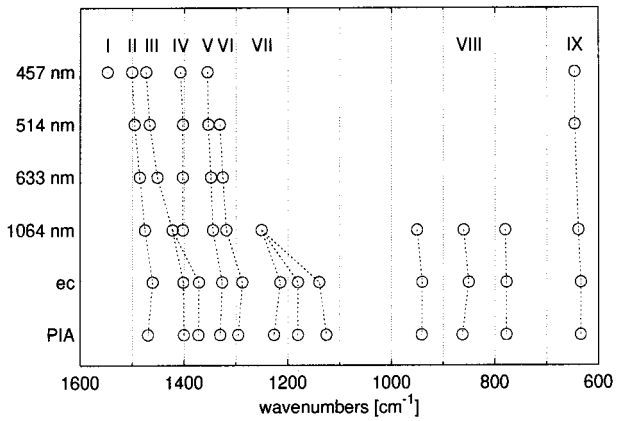

Figure 10. Outline of the Raman bands and correlation to IRAV bands of pDTT3. Roman numbers are band numbers, wavelength for Raman excitation, ec electrochemical oxidation, PIA photoinduced IR absorption.

the excitation wavelength. Moreover, almost no changes in its relative intensity and position are detected in the IR spectrum. This fact suggests that this band is associated to a localized mode in the fused rings coupled to the π-electronic system of the polymeric backbone. The localization of this mode is also indicated by the sharpness of the peak. In the Raman spectra of PTs, weak features in this spectral region were found and identified as A_g ring deformation modes containing C−S stretching.[35] Infrared bands of neutral and doped PT in the region ranging from 900 to 600 cm^{-1} have also been assigned to thiophene ring modes by several groups.[15,36−38] In pDTT3, similar contributions from C−S stretching modes localized in the two fused rings of the repeating unit, but coupled to the π-electronic system of the polymeric backbone, can be expected and are indeed found by the strong band at about 640 cm^{-1} (band IX).

The frequencies of bands I−IX are reported in Table 3. Figure 10 outlines the position of the Raman bands of the neutral polymer in dependence of the excitation wavelength and their correlation to the main IRAV modes of oxidized and photoexcited pDTT3. The HOMO of pDTT3 has been predicted "aromatic", as drawn in Figure 1a, whereas the LUMO is expected to be "quinoidal".[39] Calculations also show contributions from the median ring of the fused system that increase the antibonding character of the HOMO and slightly increase the bonding character of the LUMO.[39] Therefore, the quinoidal limiting form (Figure 1b), which, in addition, increases the aromaticity of the median ring, should have a certain weight in the electronic ground state of the polymer. This picture has two consequences:

- Less confinement of the delocalized π-electrons along the polymeric backbone into the repeating unit will be observed, as expected for a low band gap conjugated polymer like pDTT3.[18,40−42]
- Strong interaction between electron densities localized in the fused rings with the delocalized π-electrons of the polymeric backbone can be expected.

In light of this strong interaction, a splitting of bands, as observed by comparing band III in Raman and in IRAV measurements, can be expected as an effect of modulation of the high-frequency vibrations in the polymeric backbone by coupling to localized modes of the fused rings at lower frequency.

4. Conclusion

In this paper, a study of the infrared absorption spectra and of the Raman spectra in doped and undoped forms of pDTT3, a low band gap conjugated polymer, which can be reversibly electrochemically oxidized (*p*-doped) and reduced (*n*-doped), is presented. The behavior of the vibrational bands clearly indicates a coupling of vibrational modes localized on the fused ring system of the repeating unit to the delocalized electronic system of the polymer backbone. In addition, the characteristics of the IRAV bands of oxidized, reduced, and photoexcited pDTT3, which have similar high intensities and broad band shapes, show that the nature and the delocalization for both signs of the charge carriers are similar. Application of this system into optoelectronic devices such as photovoltaic cells should be promising due to the low band gap and high charge carrier delocalization for both signs of carriers.

Acknowledgment. Eitan Ehrenfreund and Teketel Yohannes are gratefully acknowledged for helpful discussions. Financial support of Austrian Foundation for Advancement of Science (FWF P-12680 CHE) is also appreciated.

References and Notes

(1) Orenstein, J. In *Handbook of Conducting Polymers*; Skotheim, T. A., Ed.; Marcel Dekker: New York, 1986; Chapter 36.
(2) Horovitz, B. *Solid State Commun.* **1982**, *41*, 729.
(3) Ehrenfreund, E.; Vardeny, Z. V.; Brafman, O.; Horowitz, B. *Phys. Rev. B* **1987**, *36*, 1535.
(4) Su, W. P.; Schrieffer, J. R.; Heeger, A. J. *Phys. Rev. Lett.* **1979**, *42*, 1698.
(5) Su, W. P.; Schrieffer, J. R.; Heeger, A. J. *Phys. Rev. B* **1980**, *22*, 2029.
(6) Zerbi, G.; Gussoni, M.; Castiglioni, C. In *Conjugated Polymers*; Brédas, J. L.; Silbey, R., Eds.; Kluwer: Dordrecht, 1991; p 435.
(7) Del Zoppo, M.; Castiglioni, C.; Zuliani, P.; Zerbi, G. In *Handbook of Conducting Polymers*, 2nd ed.; Skotheim, T. A.; Elsenbaumer, R. L.; Reynolds, J. R., Eds.; Marcel Dekker: New York, 1988; Chapter 28.
(8) Vardeny, Z.; Ehrenfreund, E.; Brafman, O.; Horovitz, B. *Phys. Rev. Lett.* **1985**, *54*, 75.
(9) Ehrenfreund, E.; Vardeny, Z. V. *Proc. SPIE* **1997**, *3145*, 324.
(10) Vardeny, Z. V.; Ehrenfreund, E.; Brafman, O.; Heeger, A. J.; Wudl, F. *Synth. Met.* **1987**, *18*, 183.
(11) Neugebauer, H.; Neckel, A.; Brinda-Konopik, N. In *Electronic Properties of Polymers and Related Compounds*; Springer Series in Solid-State Sciences, Vol. 63; Kuzmany, H.; Mehring, M.; Roth, S. Eds.; Springer: Berlin, Heidelberg, 1985; p 227.
(12) Furukawa, Y.; Akimoto, M.; Harada, I. *Synth. Met.* **1988**, *18*, 151.

(13) Louarn, G.; Mevellec, J.-Y.; Buisson, J. P.; Lefrant, S. *Synth. Met.* **1993**, *55*−*57*, 587.
(14) Mele, E. J.; Hicks, J. C. *Phys. Rev. B* **1985**, *32*, 2703.
(15) Schaffer, H. E.; Heeger, A. J. *Solid State Commun.* **1986**, *59*, 415.
(16) Agosti, E.; Rivola, M.; Hernandez, V.; Del Zoppo, M.; Zerbi, G. *Synth. Met.* **1999**, *100*, 101.
(17) Wudl, F.; Kobayashi, M.; Heeger, A. J. *J. Org. Chem.* **1984**, *49*, 3382.
(18) Roncali, J. *Chem. Rev.* **1997**, *97*, 173.
(19) Neugebauer, H.; Kvarnström, C.; Brabec, C.; Sariciftci, N. S.; Kiebooms, R.; Wudl, F.; Luzzati, S. *J. Chem. Phys.* **1999**, *110*, 24.
(20) Kvarnström, C.; Neugebauer, H.; Blomquist, S.; Ahonen, H. J.; Kankare, J.; Ivaska, A.; Sariciftci, N. S. *J. Mol. Struct.* **2000**, *521*, 271.
(21) Kvarnström, C.; Neugebauer, H.; Blomquist, S.; Ahonen, H. J.; Kankare, J.; Ivaska, A.; Sariciftci, N. S. *Synth. Met.* **1999**, *101*, 66.
(22) Arbizzani, C.; Catellani, M.; Cerroni, M. G.; Mastragostino, M. *Synth. Met.* **1997**, *84*, 249.
(23) Bolognesi, A.; Catellani, M.; Destri, S.; Ferro, D. R.; Porzio, W.; Taliani, C.; Zamboni, R. *Synth. Met.* **1989**, *28*, 527.
(24) Arbizzani, C.; Catellani, M.; Mastragostino, M.; Cerroni, M. G. *J. Electroanal. Chem.* **1997**, *423*, 23.
(25) Yassar, A.; Roncali, J.; Garnier, F. *Macromolecules* **1989**, *804*, 22.
(26) McCullough, R. D.; Lowe, R. D.; Jayaraman, M.; Anderson, D. L. *J. Org. Chem.* **1993**, *58*, 58.
(27) Chen, T.-A.; Wu, X.; Rieke, R. D. *Synth. Met.* **1993**, *175*, 60.
(28) De Jong, F.; Janssen, M. J. *J. Org. Chem.* **1971**, *36*, 1998.
(29) Neugebauer, H.; Nauer, G.; Neckel, A.; Tourillon, G.; Garnier, F.; Lang, P. *J. Phys. Chem.* **1984**, *88*, 652.
(30) Neugebauer, H.; Ping, Z. *Mikrochim. Acta* **1997**, *[Suppl.] 14*, 125.
(31) Neugebauer, H. *Macromol. Symp.* **1995**, *94*, 61.
(32) Neugebauer, H.; Sariciftci, N. S. In *Lower Dimensional Systems and Molecular Electronics*, Nato ASI series, Series B: Physics, Vol. 248; Metzger, R. M.; Day, P.; Papavassiliou G. C., Eds.; Plenum Press: New York, 1991; p 401.
(33) Gussoni, M.; Castiglioni, C.; Zerbi, G. In *Spectroscopy of Advanced Materials*; Clark, R. J. H.; Hester, R. E., Eds.; Wiley: New York, 1991; p 251.
(34) Baltchelder, D. N.; Bloor, D. In *Advances in Infrared and Raman Spectroscopy*; Clark, R. J. H.; Hester, R. E., Eds.; Wiley: **1984**, *11*, 133.
(35) Botta, C.; Luzzati, S.; Tubino, R.; Borghesi, A. *Phys. Rev. B* **1992**, *46*, 20.
(36) Hotta, S.; Shimotsuma, W.; Taketani, M. *Synth. Met.* **1984**, *10*, 85.
(37) Kobayashi, M.; Chen, J.; Chung, T.-C.; Moraes, F.; Heeger, A. J.; Wudl, F. *Synth. Met.* **1984**, *9*, 77.
(38) Moraes, F.; Davidov, D.; Kobayashi, M.; Chung, T.-C.; Chen, J.; Heeger, A. J.; Wudl, F. *Synth. Met.* **1985**, *10*, 169.
(39) Catellani, M.; Lazzaroni, R.; Luzzati, S.; Brédas, J. L. *Synth. Met.* **1999**, *101*, 175.
(40) Patil, O.; Heeger, A. J.; Wudl, F. *Chem. Rev.* **1988**, *88*, 183.
(41) Brédas, J. L. *Mol. Cryst. Liq. Cryst.* **1985**, *49*, 118.
(42) Jenekhe, S. A. *Nature* **1986**, *345*, 322.